Quasiperiodicity and revivals in dynamics of quantum phase slips in Josephson junction chains and superconducting nanowires

G. Rastelli,[1] M. Vanević,[2] and W. Belzig[1]

[1] *Fachbereich Physik, Universität Konstanz, D-78457 Konstanz, Germany*
[2] *Department of Physics, University of Belgrade, Studentski trg 12, 11158 Belgrade, Serbia*

(Dated: March 26, 2014)

Quantum phase slips in superconducting loops threaded by an external magnetic field provide a coupling between macroscopic quantum states with supercurrents circulating in opposite directions. We analyze the dynamics of the phase slips as a function of the superconducting loop length, from fully coherent dynamics for short loops to dissipative dynamics for the long ones. For intermediate lengths of the superconducting loop, the phase slips are coupled to a discrete bath of oscillators with frequencies comparable to the phase-slip amplitude. This gives rise to a quasiperiodic dynamics of the phase slips which manifests itself as a decay of oscillations between the two counterpropagating current states at short times, followed by oscillation revivals at later times. We analyze possible experimental implications of this non-adiabatic regime in Josephson junction chains and superconducting nanowires.

PACS numbers: 74.81.Fa, 74.50.+r, 85.25.Am, 74.78.Na

I. INTRODUCTION

Quantum fluctuations of the superconducting order parameter in superconductors with reduced dimensionality have attracted significant attention recently.[1–18] In nanowires, the superconducting fluctuations at low temperatures give rise to quantum phase-slip processes in which the superconductivity is locally destroyed at some instant of time while the superconducting phase across the normal part changes by $\pm 2\pi$, similarly to quantum phase-slips in Josephson junctions (see Fig. 1). A particularly challenging accomplishment is the recent experimental observation of *coherent* quantum phase slips in Josephson junction chains[1–6] and superconducting nanowires.[7–9] Coherent quantum phase slips are also the subject of intense theoretical research.[10–19] If proved feasible, coherent quantum phase slips may be used in qubits topologically protected against decoherence[20–22] and also hold promise for the realization of a fundamental current standard in quantum metrology which is dual to the Josephson voltage standard.[12,23] A possibility to realize quantum phase slips in superfluid atom circuits has been analyzed recently.[24,25]

Albeit the interest in coherent phase slips is novel, the incoherent phase slips have been studied for more than two decades already.[26–29] At finite temperature the phase slips are thermally activated, whereas at vanishing temperature they are triggered by quantum fluctuations.[30–40] Either thermal or quantum, the phase slips are *incoherent* when measured in current-biased superconducting nanowires. The incoherent phase slips occur stochastically with a *rate* $\Gamma(I)$ and during the phase slip the energy $I\Phi_0$ is dissipated into the environment, see Fig. 1(b). (Here, $\Phi_0 = h/2e$ is the flux quantum and I is the bias current.) This gives rise to a finite voltage $V = \Phi_0\Gamma(I)$ across the superconducting nanowire. Embedding the system into a superconducting loop makes a flux qubit which enables the study of coherent quantum dynamics between few quantum states, provided the system is sufficiently decoupled from external environment,[41–43] see Fig. 1(a). One of the first examples was the flux qubit made of a superconducting loop with a few Josephson junctions biased with an external magnetic flux.[1,10,44–46] In such system, the two distinguishable macroscopic states with supercurrents circulating in opposite directions exhibit coherent oscillations due to mutual coupling via quantum tunneling characterized by a quantum *amplitude* $\mathcal{V}$. A qubit made of a one-dimensional homogeneous chain of Josephson junctions has been studied recently.[13,17] Similarly, the quantum phase slips in superconducting nanowires of finite size can also exhibit coherent quantum dynamics when the wire is embedded in a superconducting loop threaded by external magnetic flux.[11,12,16]

In this paper, we study the crossover between coher-

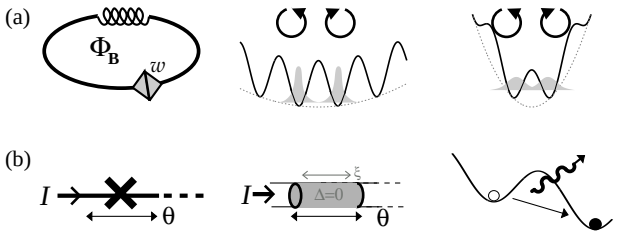

FIG. 1. (a): Phase-slip element (w) embedded into a superconducting loop makes a flux qubit (left). Effective potential is shown for inductance of the phase-slip element comparable (center) and much smaller (right) than the inductance of the loop. Phase slips coherently couple two well-defined quantum states with supercurrents circulating in opposite directions. (b): Incoherent phase slips in current-biased Josephson junctions (left) and thin superconducting nanowires (middle) correspond to $\delta\theta = \pm 2\pi$ phase changes in the effective tilted-washboard potential (right).

ent and incoherent quantum phase slips in superconducting loops as a function of the size of the system. We consider a one-dimensional ring composed of N identical Josephson junctions with an extra weak element where the phase slips take place, or, a superconducting nanowire of length L forming a loop with a weak inhomogeneity. Both systems are subject to an externally applied magnetic flux Φ_B. First, if we neglect the electrostatic interactions in the loop, the phase slips are coherent, giving rise to the change of the local phase θ across the weak element by $\pm 2\pi$. For the flux close to a half flux quantum, $\Phi_B \approx \Phi_0/2$, the phase slips coherently couple two states with supercurrents circulating in the opposite directions. The process is characterized by an amplitude $\mathcal{V}_0$ which is exponentially small in the barrier strength. Restoring the electrostatic interactions in the loop, the homogeneous part of the loop different from the phase-slip center behaves as an ensemble of harmonic oscillators, similarly to electrodynamic modes of a transmission line of a finite length. We denote the spectrum of the modes by $\{\omega_k\}$, where ω_1 is the lowest frequency which scales with the size of the system as $\omega_1 \sim 1/N$ ($\sim 1/L$). The local phase difference θ across the weak element couples to the harmonic modes which represent an effective (intrinsic) environment. We distinguish different regimes depending on the size of the system.

For small system, the frequency ω_1 may be large such that the adiabatic condition $2\mathcal{V}_0 \ll \hbar\omega_1$ holds. In this case, the dynamics of the quantum phase slips is coherent and given by the one of a two-level system, that is, it gives rise to quantum oscillations between the two supercurrent eigenstates. The effect of the high frequency modes is only the renormalization of the bare tunneling amplitude, $\mathcal{V}_0 \to \mathcal{V}$.

As the size of the system is increased, the frequencies of the low-frequency modes decrease. A resonant condition $2\mathcal{V} = \hbar\omega_1$ is met for a certain number of junctions N^* in series (length of the superconducting wire L^*), where $2\mathcal{V}$ is the energy splitting between the first excited state and the ground state of a qubit. For $N > N^*$ ($L > L^*$) the system enters the non-adiabatic regime in which some modes have frequencies smaller than the level splitting, $\hbar\omega_k < 2\mathcal{V}$ for $k = 1, \ldots, n$. In this case, the dynamics of the quantum phase slips is quasiperiodic: It exhibits decay of oscillations at short times, followed by revival of oscillations at longer times. Finally, for large system size $N \to \infty$ ($L \to \infty$), the harmonic modes form a continuous and dense bosonic bath with linear low energy dispersion. The quantum phase-slip dynamics is now dissipative and irreversible.

The remainder of the paper is organized as follows. In Sec. II, we discuss coherent phase slips in different physical systems where electrostatic interactions are neglected. In Sec. III, we analyze a simple model of a particle in a double well potential coupled to a finite discrete bath $\{\omega_k\}$ of harmonic oscillators. The dynamics of the particle has three qualitatively different regimes (coherent, quasiperiodic, and dissipative) depending on the ratio between the tunneling amplitude and the frequencies of the oscillators ($\hbar\omega_1 \gg 2\mathcal{V}$, $\hbar\omega_1 \lesssim 2\mathcal{V}$, and $\hbar\omega_1 \ll 2\mathcal{V}$, respectively). The dissipative regime is approached by increasing the density of the oscillators, that is, for the continuous bath with linear spectral function. In Sec. IV, we use the model to discuss quantum phase slips in a finite Josephson junction ring taking into account electrostatic interaction in the system. By taking the limit of large system size $N \to \infty$ and keeping the ratio Φ_B/N constant, we use our results to discuss incoherent quantum phase slips in current-biased Josephson junction chains. Similarly, in Sec. V we analyze quantum phase slips in a superconducting nanowire in a loop. In Sec. VI we present our conclusions.

II. COHERENT QUANTUM PHASE SLIPS

In this section we review different setups for studying the coherent quantum phase slips. The systems in question are superconducting loops threaded by an external magnetic flux Φ_B at temperatures much smaller than the superconducting gap, $k_B T \ll \Delta$. The effective low-energy Hamiltonian which describes the tunneling between adjacent supercurrent eigenstates reads

$$\hat{H} = \sum_m E_m |m\rangle\langle m| - \mathcal{V} \sum_m (|m+1\rangle\langle m| + \text{h.c.}), \quad (1)$$

where

$$E_m = E_L (m - \Phi_B/\Phi_0)^2 \quad (2)$$

is the energy of a state $|m\rangle$ with the supercurrent $I_m = \partial E_m/\partial\Phi_B$, and $\mathcal{V}$ is the tunneling amplitude. At fixed Φ_B, the states $|m\rangle$ are distinguishable. Below we specify E_L and $\mathcal{V}$ for different superconducting systems.

Let us consider a superconducting loop with a Josephson junction.[47,48] The potential energy of the system reads

$$V(\Phi) = (\Phi - \Phi_B)^2/2\mathcal{L} - E_J \cos(2\pi\Phi/\Phi_0), \quad (3)$$

where Φ is the flux through the loop, $\mathcal{L}$ is inductance of the loop, and $E_J = \hbar I_J/2e$ is the Josephson energy. Here, $I_J = \pi\Delta/2eR_J$ is the maximal supercurrent and R_J is the junction normal-state resistance. In the limit $E_J \gg \Phi_0^2/2\mathcal{L}$, the potential $V(\Phi)$ in Eq. (3) has well-defined minima at $\Phi \approx m\Phi_0$ (m is an integer) which correspond to the supercurrent states $|m\rangle$ with energies given by Eq. (2) and $E_L = \Phi_0^2/2\mathcal{L}$. The charging of the junction is described by a kinetic energy $C\dot{\Phi}^2/2$ where C is the junction capacitance. For $\Phi_B \approx \Phi_0/2$, the two neighboring supercurrent states are almost degenerate. They are coupled by quantum tunneling with the amplitude

$$\mathcal{V}_J = 4(8E_J^3 E_C/\pi^2)^{1/4} \exp(-\sqrt{8E_J/E_C}), \quad (4)$$

where $E_C = e^2/2C$ is the charging energy. The tunneling leads to a superposition of the counterpropagating

supercurrent states, giving rise to the anticrossing of the energy levels observed experimentally.[49] The level splitting at degeneracy point is $E_S = 2\mathcal{V}_J$.

Another system in which quantum fluctuations couple counterpropagating supercurrent states is a phase-slip flux qubit which consists of a thin superconducting nanowire. For the wire with large normal-state resistance and diameter in 10 nm range, the kinetic inductance $\mathcal{L}_k$ is much larger than the geometric inductance of the loop. In superconducting loops with wires thinner than magnetic penetration length, it is the fluxoid that is quantized rather than flux. The corresponding energies are given by Eq. (2) where $E_L = \Phi_0^2/2\mathcal{L}_k$ and $\mathcal{L}_k = m_e L/e^2 n_s A = \hbar R/\pi\Delta$. Here, m_e is the electron mass, n_s is the density of the superconducting electrons, L is the length of the wire, A is the wire cross section, and R is the wire normal-state resistance. Importantly, due to exponential sensitivity of the phase-slip amplitude $\mathcal{V}$ on the wire parameters, a *weak* inhomogeneity in the wire – where local resistivity is only *slightly* larger – will just localize the phase slips without spoiling the phase-slip character of the junction. In this case, the amplitude of the phase slips is given by

$$\mathcal{V} = \Delta\sqrt{\sum\nolimits_p T_p}\prod_p \sqrt{1-T_p}, \tag{5}$$

where T_p are spin-degenerate transmission eigenvalues that characterize the inhomogeneity.[16] Coherent quantum phase slips in nanowires have been observed recently by measuring the ensuing avoided level crossing in a junction close to degeneracy point.[7,8]

A similar situation of localized phase slips can occur in a superconducting loop made of N identical Josephson junctions in series with a weaker Josephson junction where the phase slips are pinned. The condition for this is that the phase-slip amplitude $\bar{\mathcal{V}}$ at the weak element is much larger than the one in the rest of the chain, $\bar{\mathcal{V}} \gg N\mathcal{V}_J$. [$\bar{\mathcal{V}}$ is given by an expression similar to Eq. (4), with E_J and E_C replaced by $\bar{E}_J$ and $\bar{E}_C$ of the weak element.] We note that this still allows for exponentially long chains, as long as $\bar{E}_J/\bar{E}_C \ll E_J/E_C$. When the normal-state resistance of the chain is much larger than the one of the weak element $NR_J \gg \bar{R}$ (which implies the same relation between the Josephson inductances, $\mathcal{L}_J = \hbar R/\pi\Delta$), the system is in the well-defined flux state with energy given by Eq. (2) and $E_L = \Phi_0^2/2N\mathcal{L}_J$. For $E_L \gg 2\bar{\mathcal{V}}$, the quantum phase slips effectively couple only the two neighboring supercurrent states and the system can be described by a two-level model. The supercurrent states $|m\rangle$ correspond to a phase difference $\theta \approx 2\pi m$ across the weak element. The amplitude for the phase slip $\delta\theta = \pm 2\pi$ is given by $\bar{\mathcal{V}}$ and is determined by the properties of the weak element alone.

The analysis presented so far has been carried out neglecting interactions in the loop. In the next section we develop a simple model of a particle in a double-well potential interacting with a discrete bosonic bath. Then we use the model to study dynamics of the phase slips coupled to electric modes of the loop.

III. EFFECTIVE MODEL

We consider a particle moving in a double-well potential and interacting with a bosonic bath of N harmonic oscillators, see Fig. 2. If the height of the barrier is larger than the kinetic energy $E \sim \hbar^2/ma_0^2$ of a particle localized in one of the minima positioned at $x = \pm a_0$, the system can be reduced to the localized states $|L\rangle$ and $|R\rangle$ which are coupled by quantum tunneling. This is a well-known spin-boson model[50–52] with the Hamiltonian

$$\hat{H} = \mathcal{V}_0\,\hat{\sigma}_x + \hat{\sigma}_z \sum_{k=1}^{N} \alpha_k \hbar\omega_k \left(\hat{a}_k^\dagger + \hat{a}_k\right) + \sum_{k=1}^{N} \hbar\omega_k \hat{a}_k^\dagger \hat{a}_k. \tag{6}$$

Here, $\hat{\sigma}_x = |L\rangle\langle R| + |R\rangle\langle L|$, $\hat{\sigma}_z = |L\rangle\langle L| - |R\rangle\langle R|$, $\hat{a}_k^\dagger$ ($\hat{a}_k$) are creation (annihilation) operators of the oscillator modes ω_k, α_k are the coupling constants, and $\mathcal{V}_0$ is the bare tunneling amplitude between the states $|L\rangle$ and $|R\rangle$. For large number of oscillators and linear low-frequency dispersion ($N \to \infty$, $\delta\omega \to 0$, $\omega_k = k\delta\omega$) one recovers the standard Caldeira-Leggett model[53] which describes the dissipative quantum dynamics of the two-level system coupled to an ohmic environment. This system has been studied extensively in the literature.[50–54] Here we recall the essential results which we need for further discussion. The high-energy modes with $\hbar\omega_l \gg 2\mathcal{V}_0$ quickly adjust themselves to the slow tunneling motion of the particle and hence can be treated adiabatically. These modes give rise to a renormalization of the tunneling amplitude,

$$\mathcal{V} = \mathcal{V}_0\, e^{-\sum_l \alpha_l^2/2}. \tag{7}$$

On the other hand, the low-frequency modes with linear dispersion are responsible for damping which can be characterized by a friction coefficient η. The friction results in energy dissipation $\delta E/E \sim \eta a_0^2/\hbar$ where δE is the energy dissipated during an oscillation of the particle with energy E localized in one of the wells.

In contrast to the usual dissipative case, in what follows we focus on a bath with *discrete* low-energy spectrum $\omega_k = k\delta\omega$, where the level spacing $\delta\omega$ is fixed. The adiabatic renormalization of the tunneling amplitude by

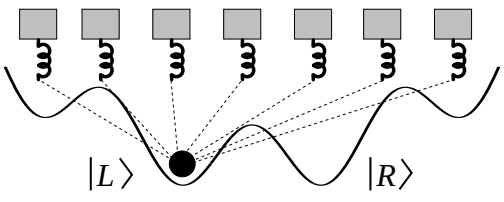

FIG. 2. Particle in a double-well potential coupled to N harmonic oscillators. States localized around the two potential minima are denoted by $|L\rangle$ and $|R\rangle$, respectively.

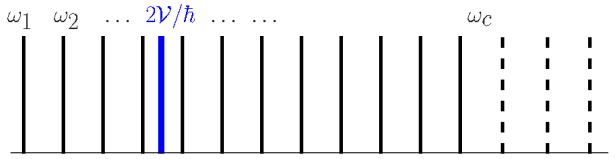

FIG. 3. (colors online) Bath energy spectrum in the non-adiabatic regime where several discrete modes have frequencies smaller or comparable to the tunnelling frequency $2\mathcal{V}/\hbar$.

high-frequency modes in Eq. (7) does not depend on the type of the bosonic bath: it is valid for a single oscillator, a discrete set of oscillators, or a continuum dense distribution.[55] On the other hand, the low frequency modes that are smaller or comparable to the tunneling amplitude are responsible for a non-adiabatic dynamics of the particle. Depending on the density of the low-frequency modes, the dynamics can be quasiperiodic for a few discrete modes or dissipative for a dense continuum of modes.

A. Non-adiabatic dynamics

Let us first separate bath the eigenmodes into the low-energy ($\omega_k < \omega_c$) and the high-energy ($\omega_k > \omega_c$) ones. The high-energy modes renormalize the bare tunneling amplitude according to Eq. (7), while the low energy modes determine the details of the particle dynamics. The choice of the cutoff frequency ω_c is nonessential provided it is much larger than the frequency of particle tunneling, $\omega_c \gg 2\mathcal{V}/\hbar$ (see Fig. 3 and Appendices A and B). In this case, the system is described by the Hamiltonian in Eq. (6) with $\mathcal{V}_0$ replaced by $\mathcal{V}$ and N replaced by N_c, where ω_k ($k = 1, \ldots, N_c$) are the low-energy modes.

Next, we apply a polaron unitary transformation $\hat{H}' = e^{\hat{\sigma}_z \hat{D}} \hat{H} e^{-\hat{\sigma}_z \hat{D}}$ with $\hat{D} = \sum_{k=1}^{N_c} \alpha_k \left(\hat{a}_k - \hat{a}_k^\dagger\right)$, in which the oscillators are displaced depending on the state of a particle. The transformed Hamiltonian reads

$$\hat{H}' = \mathcal{V}\left(\hat{\sigma}_- e^{-\hat{D}} + \hat{\sigma}_+ e^{\hat{D}}\right) + \sum_{k=1}^{N_c} \hbar\omega_k \hat{a}_k^\dagger \hat{a}_k, \qquad (8)$$

where $\hat{\sigma}_- = |L\rangle\langle R|$, $\hat{\sigma}_+ = |R\rangle\langle L|$, and we omitted an unimportant additive constant in $\hat{H}'$. For zero coupling $\hat{D} = 0$ the tunneling of the free particle is recovered ($\hat{\sigma}_- + \hat{\sigma}_+ = \hat{\sigma}_x$). The time evolution of $\hat{\sigma}_\pm$ with respect to H' is given by

$$\hat{\sigma}_\pm(t) = \hat{\sigma}_\pm(0) \pm \frac{i2\mathcal{V}}{\hbar} \int_0^t dt'\, e^{\mp \hat{D}(t')} \hat{\sigma}_z(t'). \qquad (9)$$

Substituting $\hat{\sigma}_\pm(t)$ in the equation of motion for $\sigma(t) \equiv \langle \hat{\sigma}_z(t) \rangle$, we obtain

$$\begin{aligned} \frac{d\sigma(t)}{dt} &= \frac{i\mathcal{V}}{\hbar} \left\langle e^{\hat{D}(t)} \hat{\sigma}_+(t) - \hat{\sigma}_-(t) e^{-\hat{D}(t)} \right\rangle \\ &= -\frac{4\mathcal{V}^2}{\hbar^2} \int_0^t dt'\, G(t-t')\, \sigma(t'), \end{aligned} \qquad (10)$$

where

$$G(t-t') \equiv \mathrm{Re}\left\langle e^{\hat{D}(t)} e^{-\hat{D}(t')} \right\rangle = \mathrm{Re}\left(e^{J(t-t')}\right) \qquad (11)$$

with $J(t) = -\sum_{k=1}^{N_c} \alpha_k^2 (1 - e^{-i\omega_k t})$. Here we have used the initial condition $\langle \hat{\sigma}_\pm(0) \rangle = 0$ and the noninteracting blip approximation (NIBA)[50,51,56–58] to factorize the average of a product of particle and bath operators. The approximation is based on the assumption that the dynamics of the bath is weakly perturbed by the particle ($\alpha_k^2 \ll 1$), whereas the back-action of the bath on the particle is taken into account ($\sum_k \alpha_k^2 \sim N\alpha_k^2$). Equation (10) describes the particle dynamics in a closed form for a given kernel $G(t-t')$ characterizing the bath. The kernel $G(t)$ is shown in Fig. 4 for equidistant bath frequencies $\omega_k = k\delta\omega$ and different number of modes N_c and the coupling strengths α_k. At a given coupling constant α_k, for $N_c \sim 1$, kernel $G(t)$ exhibits oscillations with a small amplitude and period $\tau_r = 2\pi/\delta\omega$ which corresponds to the revival time. Increasing the number of the modes N_c, the kernel $G(t)$ decays at short times with a time constant $(\sum_k \alpha_k^2 \omega_k^2/2)^{-1/2}$ which corresponds to the typical duration of the revivals occurring after a period τ_r. To complete the analysis, we note that $G(t)$ has also another time scale τ_s for high cut-off N_c, associated with the fast oscillations inside the duration of one revival, with frequency $\sim \sum_k \alpha_k^2 \omega_k$.

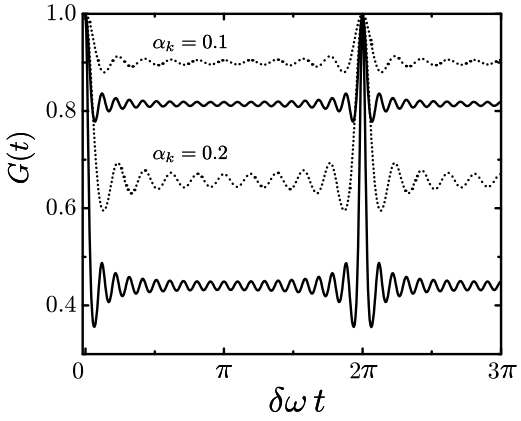

FIG. 4. The kernel $G(t)$ for the bath with $N_c = 10$ modes (dotted) and $N_c = 20$ modes (solid curve) and the coupling strength $\alpha_k = 0.1$ (top) and $\alpha_k = 0.2$ (bottom). The frequencies of the modes are assumed equidistant, $\omega_k = k\delta\omega$.

In what follows we solve Eq. (10) assuming equidistant low-energy spectrum of the bath $\omega_k = k\delta\omega$ ($k = 1, \ldots, N_c$). Taking the Laplace transform of Eq. (10) we

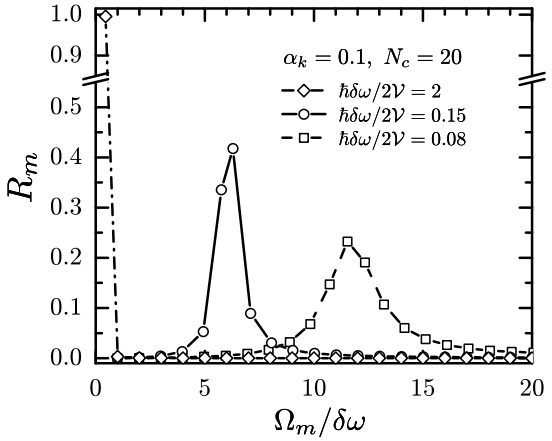

FIG. 5. Frequency spectrum for a particle coupled to a bath of $N_c = 20$ modes with $\alpha_k = 0.1$ and the level spacing $\hbar\delta\omega/2\mathcal{V} = 2$ (diamonds), 0.15 (circles), and 0.08 (squares).

obtain

$$\sigma(s) = \frac{\sigma_0}{s + (4\mathcal{V}^2/\hbar^2)G(s)} \tag{12}$$

where $\sigma_0 \equiv \sigma(t=0)$ and $G(s) = \sum_{m=0}^{\infty} c_m s/(s^2+\omega_m^2)$. The coefficients c_m are given by

$$c_m = e^{-\sum_k \alpha_k^2} \sum_{\{k\}}{}' \frac{\alpha_1^{2k_1}\alpha_2^{2k_2}\cdots\alpha_{N_c}^{2k_{N_c}}}{k_1!k_2!\cdots k_{N_c}!} \tag{13}$$

where $'$ denotes summation over $k_n \geq 0$ with constraint $\sum_{n=1}^{N_c} nk_n = m$. The constraint takes into account the degeneracy of the energy eigenstate $\hbar\omega_m$ of the bath. Coefficients c_m obey the sum rule $\sum_{m=0}^{\infty} c_m = 1$.

Equation (12) has poles at $s = \pm i\Omega_m$, where $\omega_m < \Omega_m < \omega_{m+1}$ $(m = 0, 1, \ldots)$. Taking the inverse Laplace transform of Eq. (12) we obtain

$$\sigma(t) = \sigma_0 \sum_{m=0}^{M} R_m \cos(\Omega_m t) \tag{14}$$

with $R_m = \prod_{n=1}^{M}(\omega_n^2 - \Omega_m^2)/\prod_{n=0}^{\prime M}(\Omega_n^2 - \Omega_m^2)$. Here, $'$ denotes that the term with $n = m$ is omitted in the denominator of R_m and M is a cutoff chosen sufficiently large such that convergence is achieved.

A crossover from adiabatic to non-adiabatic dynamics is shown in Figs. 5 and 6 for a particle coupled to a bath with $N_c = 20$ modes, $\alpha_k = 0.1$, and the level spacing $\hbar\delta\omega/2\mathcal{V} = 2$, 0.15, and 0.08, respectively. The average position of a particle $\sigma(t)$ is shown in Fig. 6. In the adiabatic case $\hbar\delta\omega/2\mathcal{V} = 2$, we observe in Fig. 5 that only the lowest frequency is relevant. It is approximately equal to the renormalized frequency given by Eq. (7) with the sum including all the modes (see Appendix A). In this case the dynamics corresponds simply to coherent oscillations shown Fig. 6(a). As the density of the modes is increased, several frequencies Ω_m start to contribute,

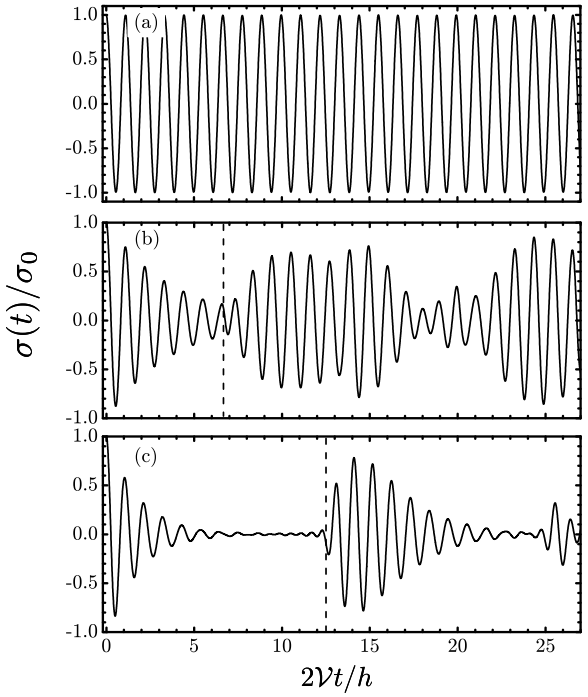

FIG. 6. Average position $\sigma(t)$ for a particle coupled to a discrete bath with $N_c = 20$, $\alpha_k = 0.1$, and the level spacing (a) $\hbar\delta\omega/2\mathcal{V} = 2$, (b) $\hbar\delta\omega/2\mathcal{V} = 0.15$, and (c) $\hbar\delta\omega/2\mathcal{V} = 0.08$. The corresponding frequency spectra are shown in Fig. 5. Dashed lines in (b) and (c) indicate the onset of revivals at $t = 2\pi/\delta\omega$.

with amplitudes R_m shown in Fig. 5. In the weak coupling regime which we consider, the particle still oscillates between the two minima with the frequency $2\mathcal{V}/\hbar$ corresponding to the fast oscillations in Figs. 6(b) and (c). The amplitude of these oscillations initially decays as the bath modes are populated and the energy is transferred from the particle to the bath. The decay time is $\tau_d \propto \hbar^2/\mathcal{V}^2\sqrt{(\sum_k \alpha_k^2\omega_k^2)/(\sum_k \alpha_k^2)}$. However, after time $\tau_r = 2\pi/\delta\omega$, the populated bath modes start to feed energy back to the particle and revivals of oscillations take place. From that point on, we have two different behaviors depending on the ratio τ_d/τ_r. For $\tau_d \lesssim \tau_r$, the dynamics of a particle has a form of a quasiperiodic beating instead of a decay. Reducing $\tau_d \ll \tau_r$, the dynamics exhibits again a decay after a revival of the oscillation amplitude. For a dense continuum of bath modes ($N_c \to \infty$, $\delta\omega \to 0$) the revival time is infinite, $\tau_r \to \infty$. In this case the bath cannot feed significant amounts of energy back to the particle and one recovers exponentially damped oscillations characteristic for Ohmic dissipation.

IV. JOSEPHSON JUNCTION RING WITH A WEAK ELEMENT

Here we study quantum phase slips in a superconducting ring which consists of N identical Josephson junctions and a weaker Josephson junction at which the phase slips

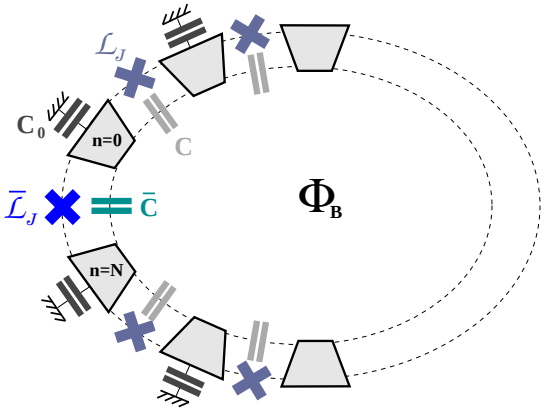

FIG. 7. (colors online) Superconducting ring made of N identical Josephson junctions with inductances $\mathcal{L}_J$ and capacitances C, and a weaker Josephson junction with inductance $\bar{\mathcal{L}}_J$ and capacitance $\bar{C}$. Ground capacitance of the superconducting islands between the junctions is C_0.

are localized, see Fig. 7. We show how the dynamics of the quantum tunneling between the two counterpropagating supercurrent states discussed in Sec. II can be mapped to the spin-boson model of Sec. III when the electric modes of the ring are taken into account.

Let ϕ_n be the superconducting phases of $N+1$ islands forming the ring. Under the conditions discussed in Sec. II, the quantum phase slips mainly occur at the weak junction whereas the other N junctions behave as inductances $\mathcal{L}_J = \Phi_0^2/4\pi^2 E_J$. This implies that the phase-differences $\delta\phi_n = \phi_{n+1} - \phi_n$ $(n = 0, \ldots, N-1)$ across the Josephson junctions in the ring remain small as compared to 2π and oscillate around their average values. On the other hand, the phase difference $\theta = \phi_0 - \phi_N$ across the weak junction can make a 2π winding. In this regime, the corresponding Euclidean Lagrangian of the system reads[17,59,60]

$$\mathscr{L} = \frac{\hbar^2\dot{\theta}^2}{16\bar{E}_C} - \bar{E}_J\cos(\theta+\delta_B) + \sum_{n=0}^{N-1}\left(\frac{\hbar^2(\delta\dot{\phi}_n)^2}{16E_C} + \frac{E_J}{2}(\delta\phi_n+\delta_B)^2\right) + \sum_{n=0}^{N}\frac{\hbar^2\dot{\phi}_n^2}{16E_0}, \tag{15}$$

where $E_0 = e^2/2C_0$ is the charging energy of the islands and $\delta_B = 2\pi(\Phi_B/\Phi_0)/(N+1)$ is the phase increment due to external magnetic field.

Next we cast Eq. (15) in the form in which the coupling of θ to electric modes of the ring is manifest.[17] We take as independent variables the phases between Josephson junctions, $\varphi_n \equiv \phi_n$ for $n = 1, \ldots, N-1$, the average phase $\varphi_0 \equiv (\phi_0 + \phi_N)/2$ and the phase difference θ across the weak element. Since φ_n is periodic on the effective lattice $n = 0, \ldots, N-1$ composed of N elements, it can be Fourier transformed as $\varphi_n = (1/\sqrt{N})\sum_{k=0}^{N-1}\varphi_k \exp(i2\pi nk/N)$ where $\varphi_{N-k} = \varphi_k^*$. The real and imaginary parts φ_k' and φ_k'' of φ_k give rise to even and odd modes, respectively. After the substitution in Eq. (15), we find that only φ_k'' couple to θ while φ_k' describe a set of decoupled harmonic oscillators.[17] Since $\varphi_{N-k}'' = -\varphi_k''$, only half of the modes are independent; we denote these modes as $X_k \equiv \varphi_k''$ for $1 \le k \le k_{\max}$, where $k_{\max} = \lfloor (N-1)/2 \rfloor$ and $\lfloor x \rfloor$ is the integer part of x. The Lagrangian of the system reads $\mathscr{L} = \mathscr{L}_0 + \mathscr{L}_{\rm int}$ where

$$\mathscr{L}_0 = \frac{\hbar^2\dot{\theta}^2}{16E_{\tilde{C}}} - \bar{E}_J\cos(\theta+\delta_B) + E_L(\theta - N\delta_B)^2/4\pi^2 \tag{16}$$

and

$$\mathscr{L}_{\rm int} = \sum_{k=1}^{k_{\max}}\left[\frac{\mu_k}{2}\left(\dot{X}_k - \frac{f_k\dot{\theta}}{\mu_k}\right)^2 + \frac{\mu_k\omega_k^2}{2}\left(X_k - \frac{g_k\theta}{\mu_k\omega_k^2}\right)^2\right]. \tag{17}$$

The Lagrangian $\mathscr{L}_0$ describes the phase θ in a double-well potential with two degenerate minima at half flux quantum ($N\mathcal{L}_J \gg \bar{\mathcal{L}}_J$, where $N\mathcal{L}_J$ is the effective inductance of the ring; $E_L \equiv \Phi_0^2/2N\mathcal{L}_J$). The minima correspond to the counterpropagating supercurrent states that enter the spin-boson model (cf. Sec. III and Fig. 2) and which are coupled by the phase slips.[1,13,17] Josephson junctions in the chain give rise to a renormalization of the charging energy of the weak element $E_{\tilde{C}} = e^2/2\tilde{C}$, where

$$\tilde{C} = \bar{C} + \frac{C}{N} + \frac{C_0}{2}\left(1 + \frac{1}{N}\sum_{k=1}^{k_{\max}}\frac{\cos^2(\pi k/N)}{\sin^2(\pi k/N) + C_0/4C}\right). \tag{18}$$

The term $\mathscr{L}_{\rm int}$ in Eq. (17) describes the electric modes in the ring and their interaction with θ. The dispersion of the modes reads

$$\omega_k = \frac{\omega_p\sin(\pi k/N)}{\sqrt{\sin^2(\pi k/N) + C_0/4C}} \tag{19}$$

with $\omega_p = 1/\sqrt{\mathcal{L}_J C}$, $\mu_k = (8E_J/\omega_k^2)\sin^2(\pi k/N)$, and $g_k = \omega_p^2 f_k = (2E_J/\sqrt{N})\sin(2\pi k/N)$. Note that interaction in Eq. (17) does not confine θ because it depends on the relative coordinates with respect to the bath degrees of freedom.

A. Real-time dynamics

The harmonic modes of the ring can be integrated out using the Feynman-Vernon influence functional in the real-time path integral approach. The resulting influence action which governs the dynamics of θ is a functional of the spectral density of the modes

$$F(\omega) = \frac{\hbar}{\pi}\sum_k \alpha_k^2\omega_k^2\delta(\omega - \omega_k). \tag{20}$$

Thus, the linear coupling of the phase difference θ at the weak element to an ensemble of harmonic oscillators affects the dynamics of θ only through $F(\omega)$, regardless the details of the bath.[50,51] Hence, from the knowledge of the coupling constants α_k and the spectrum ω_k one can analyze the real-time dynamics of the quantum tunneling between the two low-energy states in a double-well potential of Eq. (16) using the effective spin-boson model as described in Sec. III.

Instead of carrying out calculation in the real-time formalism, we can proceed with the imaginary-time one and make use of a relation[51]

$$K_l = \frac{2}{\pi}\int_0^\infty d\omega \frac{\nu_l^2 F(\omega)}{\omega(\nu_l^2+\omega^2)} = \frac{2\hbar}{\pi^2}\sum_k \alpha_k^2 \frac{\nu_l^2\omega_k}{\nu_l^2+\omega_k^2} \qquad (21)$$

between $F(\omega)$ and the kernel $K_l = K(\nu_l)$ of the imaginary-time effective action ($\nu_l = 2\pi l/\tau_0$ are the Matsubara frequencies and τ_0 is the time-interval in the imaginary time axis). The latter can be obtained from the partition function of the system which is given by imaginary-time path integral over closed trajectories $\theta(0) = \theta(\tau_0)$ and $X_k(0) = X_k(\tau_0)$:

$$\mathcal{Z}_{\rm tot} = \oint \mathcal{D}\theta\mathcal{D}X\, e^{-(S_0+S_{\rm int})/\hbar}, \qquad (22)$$

where $S_0[\theta] = \int_0^{\tau_0} d\tau \mathscr{L}_0[\theta]$ and $S_{\rm int}[\theta, X] = \int_0^{\tau_0} d\tau \mathscr{L}_{\rm int}[\theta, X]$. After integrating out bath degrees of freedom, one obtains $\mathcal{Z}_{\rm tot} = \mathcal{Z}_h \times \mathcal{Z}$, where $\mathcal{Z}_h = \prod_k [2\sinh(\omega_k\tau_0/2)]^{-1}$ is the partition function of harmonic oscillators and

$$\mathcal{Z} = \oint \mathcal{D}\theta\, e^{-(S_0+S_{\rm inf})/\hbar} \qquad (23)$$

is the partition function of the particle interacting with the bath. The interaction is included in the influence action

$$S_{\rm inf}[\theta] = \frac{1}{2}\int_0^{\tau_0} d\tau d\tau' \theta(\tau)K(\tau-\tau')\theta(\tau') = \frac{1}{\tau_0}\sum_{l=1}^{\infty} K_l|\theta_l|^2, \qquad (24)$$

where $\theta_l = \int_0^{\tau_0} d\tau\, \theta(\tau) e^{i\nu_l\tau}$.

After integration of the harmonic modes in $\mathscr{L}_{\rm int}$, we obtain

$$S_{\rm inf} = \frac{1}{\tau_0}\sum_{l=1}^{\infty}|\theta_l|^2 \sum_{k=1}^{k_{\rm max}} \frac{\nu_l^2}{\nu_l^2+\omega_k^2}\frac{g_k^2}{\mu_k\omega_k^2}\left(1-\frac{\omega_k^2}{\omega_p^2}\right)^2, \qquad (25)$$

and using Eqs. (21) and (24) we extract the coupling constants:

$$\alpha_k = \frac{\pi}{\sqrt{N}}\left(\frac{E_J}{\hbar\omega_k}\right)^{1/2}\left(1-\frac{\omega_k^2}{\omega_p^2}\right)\cos(\pi k/N). \qquad (26)$$

Note that the ground capacitance plays a crucial role: For $C_0 = 0$ the dispersion relation becomes flat with $\omega_k = \omega_p \gg 2\bar{\mathcal{V}}/\hbar$ and the only effect of the ring is the adiabatic confining potential associated with the ring's inductance, see Eq. (16).[17]

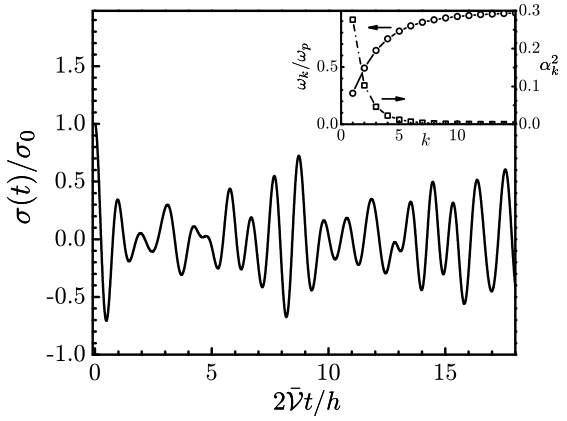

FIG. 8. Non-adiabatic dynamics of a phase-slip qubit made of a Josephson junction chain with a weak element. Parameters are $\bar{C}/C = 0.1$, $C_0/C = 0.05$, $Z_J/R_q = 0.18$, $N = 100$, and $\hbar\omega_p/\bar{\mathcal{V}} = 3$. Inset: Dispersion ω_k (circles, left axis) and the coupling constants α_k^2 (squares, right axis) of the modes in the chain.

Next we focus on the regime $N \gg \omega_0/\omega_p$ ($\omega_0 = 1/\sqrt{\mathcal{L}_J C_0}$) in which the maximum frequency $\omega_{k_{\rm max}} \approx \omega_p$ and dispersion at low frequencies is linear, $\omega_k \approx (2\pi k/N)\omega_0$. The coupling constants at low frequencies are given by

$$\alpha_k = \frac{1}{2}\sqrt{\frac{R_q}{Z_0}}\frac{1}{\sqrt{k}} \qquad (k < N_c), \qquad (27)$$

where $R_q = h/4e^2$ is the quantum resistance and $Z_0 = \sqrt{\mathcal{L}_J/C_0}$ is the low-frequency transmission-line impedance of the ring. The cutoff frequency $\omega_c = \omega_{k=N_c}$ with $\sin(\pi N_c/N) = \sqrt{C_0/4C}$ discriminates between a linear (low-frequency) and a nonlinear (high-frequency) part of the spectrum. As long as $2\bar{\mathcal{V}} < \hbar\omega_p$, this frequency also divides the low-frequency modes responsible for the details of the phase dynamics from the high-frequency modes which only renormalize the phase slip amplitude.

In the following we analyze the feasibility of achieving a non-adiabatic phase-slip dynamics in realistic superconducting rings made of Josephson junctions. Since capacitance of the junction is proportional to the cross section-area while inductance is inversely proportional to it, we have $\mathcal{L}_J C = \bar{\mathcal{L}}_J \bar{C}$. In this case, the condition $N\mathcal{L}_J \gg \bar{\mathcal{L}}_J$ for the system to be in a well-defined flux state implies $\bar{C} \gg C/N$ and the renormalization of the capacitance of the weak element in Eq. (18) is negligible. The hierarchy of energy scales $N\mathcal{V}_J \ll \bar{\mathcal{V}} \ll E_L$ discussed in Sec. II gives the upper limit of the ring length, $N \ll N_a, N_b$, where $N_a = \sqrt{\mathcal{L}_J/\bar{\mathcal{L}}_J}\exp[(4/\pi)R_q(Z_J^{-1} - \bar{Z}_J^{-1})]$ and $N_b \approx 3.5(\bar{\mathcal{L}}_J/\mathcal{L}_J)\sqrt{R_q/Z_J}\exp[(4/\pi)R_q/\bar{Z}_J]$ with $Z_J = \sqrt{\mathcal{L}_J/C}$ and $\bar{Z}_J = \sqrt{\bar{\mathcal{L}}_J/\bar{C}}$. These conditions are not very restrictive and can be met in realistic de-

vices, as demonstrated experimentally in the fluxonium superconducting chain with $N = 43$ Josephson junctions in series.[4] In addition to the previous conditions, for non-adiabatic phase dynamics to occur the lowest frequency of electric modes has to be smaller than the qubit level splitting, $\hbar\delta\omega = 2\pi\hbar\omega_0/N < 2\bar{\mathcal{V}}$. This can be achieved, e.g., by making the ground capacitance larger than a certain threshold, $C_0 > (\pi\hbar/N\bar{\mathcal{V}})^2\mathcal{L}_J^{-1}$. Experimentally, the capacitance C_0 should not be too large in order to reduce decoherence caused by charge fluctuations in the environment.

As an example, we take $N = 100$ junctions in series, $\bar{C}/C = 0.1$, $C_0/C = 0.05$, and $Z_J/R_q = 0.18$. The dispersion of the modes and the coupling constants are given by Eqs. (19) and (26), respectively (see inset of Fig. 8). The non-adiabatic dynamics of the qubit is shown in Fig. 8 obtained by numerical simulation of Eq.(10). The dynamics exhibits the same qualitative features (initial decay and revivals) as discussed in Sec. III for a generic model with equidistant spectrum of the modes and constant coupling of the phase to the bath degrees of freedom. Increasing the number of junctions or the strength of the coupling α_k (e.g., by increasing the capacitance C_0 to the ground), the number of electric modes that are coupled to the phase increases and the transition from coherent non-adiabatic to fully incoherent dynamics takes place. Recent experiments reported the fabrication of long Josephson junction chains comparable in order of magnitude to our example and operating as linear "superinductance" elements in which quantum phase slips are suppressed.[61] In addition, Josephson junction chains in the ladder geometry have been studied experimentally.[62] In this system, quantum phase slips are prevented at the topological level which opens the route towards realization of long Josephson junction chains behaving as perfect inductances.

B. Thermodynamic limit and incoherent dynamics

Let us consider a Josephson junction ring with a large number of junctions N and large external flux Φ_B such that the ratio $I = \Phi_B/N\mathcal{L}_J$ is finite. The Eq.(16) becomes

$$\mathscr{L}_0 = \frac{\hbar^2\dot{\theta}^2}{16E_{\tilde{C}}} - \bar{E}_J\cos(\theta) - \Phi_0 I\theta/2\pi, \qquad (28)$$

where, without loss of generality, we performed a phase shift $\theta \to \theta - \delta_B$ and omitted an unimportant additive constant. The Lagrangian $\mathscr{L}_0$ in Eq. (28) describes current-biased Josephson junction with the phase θ moving in a tilted washboard potential, see Fig. 1(b). The interaction of θ with electric modes of the ring is given by Eq. (17). For large number of junctions N, the low-frequency modes $\omega_k = (2\pi k/N)\omega_0$ ($\omega_k < \omega_c$) form a quasicontinuum with linear spectral density $F(\omega) = (R_q/4\pi Z_0)\hbar\omega$ and kernel $K_l = F(\nu_l)$, see Eqs. (20) and (21). Since the kernel is linear in frequency, the resulting influence action in Eq. (24) corresponds to an ohmic dissipative environment.

For large energy barrier $\bar{E}_J \gg E_{\tilde{C}}$, small tilting $I/2e \ll \omega_p$, and in the presence of dissipation, the phase is strongly localized in the potential minima. In this regime, at finite temperature, the dynamics of the phase consists of incoherent hopping between the neighboring minima with energy difference $\Phi_0 I$ which is emitted to or absorbed from the environment, cf. Fig 1(b).[63–65] The phase change $\delta\theta = \pm 2\pi$ occurs with the rate $\Gamma_\pm = \Gamma(\pm\Phi_0 I)$. The average phase evolves as $d\theta/dt = 2\pi(\Gamma_+ - \Gamma_-)$, giving rise to the voltage $V = \Phi_0[\Gamma_+(I) - \Gamma_-(I)]$ across the junction. From a two-level Hamiltonian in Eq. (8) and using the perturbation theory for tunneling between the levels,[50] one obtains the rate $\Gamma_\pm = (\bar{\mathcal{V}}/\hbar)^2\int_{-\infty}^{\infty} dt\exp[J(t) \mp i\Phi_0 It/\hbar]$ where the correlation function $J(t) = \langle\hat{D}(0)[\hat{D}(t) - \hat{D}(0)]\rangle_T$ is evaluated for the harmonic bath at thermal equilibrium. This is the so-called *dual* $P(E)$ theory for incoherent quantum phase-slips.[66] The correlation function $J(t)$ has a universal long-time behavior[63–65] $J(t) \approx -2(R_q/Z_0)\{\ln[(\hbar\omega_p/\pi k_B T)\sinh(\pi k_B T t/\hbar)] + i\mathrm{sgn}(t)\pi/2\}$ (hereafter we set $k_B = 1$). At low temperatures $T \ll \hbar\omega_p(Z_0/R_q)$, the universal limit of $J(t)$ is valid for all times and the rates $\Gamma_\pm$ can be evaluated analytically. For the average voltage across the junction we recover[67]

$$V \approx \frac{2\Phi_0\bar{\mathcal{V}}^2}{\hbar^2\omega_p}\left(\frac{2\pi T}{\hbar\omega_p}\right)^{2g-1}\frac{|\Gamma(g + \frac{i\Phi_0 I}{2\pi T})|^2}{\Gamma(2g)}\sinh\left(\frac{\Phi_0 I}{2T}\right), \qquad (29)$$

where $g = R_q/Z_0$ and $\Gamma(x)$ is the Euler gamma function.

V. SUPERCONDUCTING NANOWIRE WITH A WEAK LINK

Quantum phase slips in a superconducting nanowire can be pinned at a weak inhomogeneity where the local resistivity is slightly increased. The inhomogeneity can be modelled as a weak link with the action which is nonlocal in time.[16] This leads to the bare phase-slip amplitude $\mathcal{V}$ in Eq. (5), in contrast to the case of a Josephson junction ring in which $\mathcal{V}$ is given by Eq. (4) (with E_J and E_C replaced by $\bar{E}_J$ and $\bar{E}_C$ of the weak element). The effect of the nanowire on quantum phase slips can be taken into account by modelling the wire as an LC transmission line.[68] With no external magnetic field applied, the action of the wire reads

$$S_{\mathrm{w}}[\phi] = \frac{1}{\tau_0}\sum_{l=-\infty}^{\infty}\left(\frac{\hbar}{2e}\right)^2\int_0^L dx\left(\frac{1}{2\mathcal{L}'(\nu_l)}|\partial_x\phi(\nu_l,x)|^2 + \frac{C_0'\omega^2}{2}|\phi(\nu_l,x)|^2\right). \qquad (30)$$

Here, L is the length of the wire, $\phi(\nu,x)$ is the superconducting phase along the wire, C_0' is the capacitance to

the ground, and $\mathcal{L}'(\omega)$ is the imaginary-frequency inductance which is obtained by analytic continuation of the impedance,[69] $\mathcal{L}'(\omega) \equiv Z'_s(-i|\omega|)/|\omega|$. (Prime $'$ denotes quantities defined per unit length.) The impedance is $Z'_s(\omega) = R'\sigma_n/\sigma(\omega)$, where σ_n is the normal-state conductivity and $\sigma(\omega) = \sigma_1(\omega) - i\sigma_2(\omega)$ is the complex conductivity of a diffusive superconductor. At zero temperature, the real and imaginary parts $\sigma_{1,2}(\omega)$ are given by[70] $\sigma_1(\omega)/\sigma_n = (1 + 2\Delta/\hbar\omega)E(\kappa) - (4\Delta/\hbar\omega)K(\kappa)$ for $\omega > 2\Delta/\hbar$, and $\sigma_1(\omega) = 0$ otherwise, and $\sigma_2(\omega)/\sigma_n = (1 + 2\Delta/\hbar\omega)E(\kappa')/2 - (1 - 2\Delta/\hbar\omega)K(\kappa')/2$ for $\omega > 0$, where $\kappa = (\hbar\omega - 2\Delta)/(\hbar\omega + 2\Delta)$, $\kappa' = \sqrt{1-\kappa^2}$, and K, E are the complete elliptic integrals of the first and the second kind, respectively. Analytic continuation $\sigma(-i|\omega|)$ is performed separately in domains $|\omega| < 2\Delta/\hbar$ and $|\omega| > 2\Delta/\hbar$. The resulting $\mathcal{L}'(\omega)$ is real and even function of frequency, continuous at $\omega = 2\Delta/\hbar$, with $\mathcal{L}'(\omega) = \mathcal{L}'_k[1-(\hbar\omega/4\Delta)^2]$ for $\omega \ll 2\Delta/\hbar$ ($\mathcal{L}'_k \equiv \hbar R'/\pi\Delta$), and $\mathcal{L}'(\omega) = R'/\omega$ for $\omega \gg 2\Delta/\hbar$. Thus, at subgap frequencies the wire is inductive with kinetic inductance $\mathcal{L}'_k$,[68] while at frequencies much larger than the gap it acts as an ohmic resistance R'. Since the phase-slip amplitude $\mathcal{V} \ll \Delta$, we can set $\mathcal{L}'(\nu) = \mathcal{L}'_k$ in Eq. (30). From Eq. (15) it follows that the wire can be mapped into a chain of Josephson junctions with inductances $\mathcal{L}_J = \mathcal{L}'_k L/N$, capacitances to the ground $C_0 = C'_0 L/N$, and $C = 0$. In particular, low-frequency modes in the wire have dispersion $\omega_k = 2\pi k/L\sqrt{\mathcal{L}'_k C'_0}$ with the coupling constants given by Eq. (27), where Z_0 is replaced by impedance of the wire $Z_{\rm w} = \sqrt{\mathcal{L}'_k/C'_0}$. If RC time of the wire is large, $\tau_{RC} = L^2 R' C'_0 \gg \hbar\Delta/\mathcal{V}^2$, the system may enter a non-adiabatic regime discussed in Sec. III and IV in which the phase dynamics is quasiperiodic.

VI. CONCLUSION

In conclusion, we have studied quasiperiodic quantum dynamics and revivals between two macroscopic supercurrent states in superconducting one-dimensional rings with a weak element and threaded by a magnetic field. At half flux quantum, such systems are a canonical example of persistent current or flux qubits.[1,11] We have discussed possible realizations of such systems in the form of a Josephson junctions chain and a superconducting nanowire forming a loop.

Two collective states with supercurrents circulating in opposite directions are associated to 0 and 2π phase difference across the weak element. For sufficiently large system size, we have found that the quantum dynamics can be more complex than the usual coherent oscillations between the two states, characterized by the quantum phase-slip amplitude $\mathcal{V}$. Such a dynamics emerges due to the intrinsic electrostatic interactions in the homogeneous part of the ring. This gives rise to electrodynamic modes with linear low-frequency dispersion which couple to the phase. We have obtained the spectrum of the modes and the coupling strength to the phase drop at the phase-slip element as a function of the system parameters. We have discussed the experimental feasibility to observe the quasiperiodic dynamics in realistic systems, in the regime in which only a few low-energy modes with frequencies less than or comparable to $2\mathcal{V}$ are effectively coupled to the phase. In the non-adiabatic regime, dynamics of the system is quasiperiodic with exponential decay of oscillations at short times followed by oscillation revivals at later times. This is a cross-over regime between coherent dynamics discussed in flux qubits and incoherent phase-slip processes in current-biased junctions or superconducting wires coupled to external dissipative environment. In our scheme, the incoherent regime is recovered for large system size ($N, L \to \infty$), provided the electric modes are decoupled from the external environment.

Recent experiments have shown that a larger number of degrees of freedom is not necessarily penalized by decoherence,[5,71–73] opening the possibility to explore novel dynamic regimes beyond the two-level's one. Therefore, observation of a quasiperiodic dynamics would be important for understanding the mechanisms of decoherence in large quantum circuits as well as intrinsic limits on coherence posed by the circuit itself. Our results can also be of interest for the design of models with a tunable fictitious dissipation or, for instance, to achieve controlled quantum evolution in superconducting qubits by engineering the parameters of the Josephson junction circuits. This motivates future studies of flux qubits realized in large superconducting circuits with a more complex topological structure.[62] The approach we use is not restricted to superconducting circuits and can be readily generalized for other situations in which the intrinsic bosonic degrees of freedom couple to the phase, like in quasi-1D superfluid condensates.[24,25]

ACKNOWLEDGMENTS

The research was supported by the EU FP7 Marie Curie Zukunftskolleg Incoming Fellowship Programme, University of Konstanz (grant No. 291784). M.V. acknowledges support by the Serbian Ministry of Science, project No. 171027.

Appendix A: Phase dynamics and the adiabatic regime

Here we analyze the relation between the adiabatic renormalization of the amplitude in Eq. (7) and the time dynamics of the phase given by Eq. (10). Let us start with the bare Hamiltonian in Eq. (6) in the regime in which all the frequencies satisfy the adiabatic condition $\hbar\omega_1 = \hbar\delta\omega \gg 2\mathcal{V}_0$. Then, by applying the same steps of Sec. III A, we obtain Eq. (12) with $\mathcal{V}_0$ replacing $\mathcal{V}$ and for

N harmonic oscillators. At low $s \ll \delta\omega < \omega_m$ (long time intervals), we can approximate $G(s)$ in the denominator of Eq. (12) by its first term:

$$\frac{\sigma(s)}{\sigma_0} \approx \frac{1}{s + (4\mathcal{V}_0^2/\hbar^2)c_0/s} = \frac{s}{s^2 + 4\mathcal{V}^2/\hbar^2}\,, \qquad \text{(A1)}$$

where $c_0 = \exp(-\sum_{k\geq 1}\alpha_k^2)$. Thus, there is a single pole $2\mathcal{V}/\hbar$ at low-frequencies (see Fig. 5 for $\hbar\delta\omega/2\mathcal{V} = 2$) whereas the other poles are relevant only at higher frequencies ($\sim \delta\omega$). In the time domain, Eq. (A1) corresponds to an oscillatory two-levels evolution with a renormalized frequency $2\mathcal{V}/\hbar$ as compared to the bare frequency in Eq. (6) and we recover the adiabatic phase dynamics.

Appendix B: Dependence on the cut-off N_c

Now we demonstrate that the solution associated to the effective spin-boson model in Eq. (8) corresponds to the low-frequency solution of the bare spin-boson system in Eq. (6) and that such a solution is independent of the high-frequency cut-off ω_c provided that ω_c is chosen sufficiently large $\omega_c \gg \delta\omega \sim \mathcal{V}$. This is equivalent to show that the product $\mathcal{V}^2 G(s)$ in Eq. (10) does not change at low-frequencies $s \ll \omega_c$.

First, we shift the cut-off $\omega_c' = \omega_c + \delta\omega$, namely $N_c' = N_c + 1$, so that we have to re-scale all the parameters accordingly. Recalling that $\mathcal{V}/\mathcal{V}_0 = \exp(-\sum_{k=N_c+1}^{\infty}\alpha_k^2/2)$, we obtain for the renormalized amplitude

$$\mathcal{V}' = \mathcal{V}\exp(\alpha_{N_c+1}^2/2)\,, \qquad \text{(B1)}$$

whereas for the coefficients c_m we have

$$c_m' = e^{-\sum_{k=1}^{N_c+1}\alpha_k^2} \sum_{\{k\}}{}' \frac{\alpha_1^{2k_1}\alpha_2^{2k_2}\cdots\alpha_{N_c+1}^{2k_{N_c+1}}}{k_1!k_2!\cdots k_{N_c+1}!}\,, \qquad \text{(B2)}$$

with the new constraint $\sum_{n=1}^{N_c+1} nk_n = m$. Importantly we notice that, for every m such that $m \leq N_c$, the sum for the two sets of coefficients $\{c_m\}$ and $\{c_m'\}$ satisfies the same constraint because the term $n = N_c + 1$ is not involved in Eq. (B2) as it can not satisfy the constraint $nk_n = N_c$ for any integer k_n. Therefore, we have simply

$$c_m' = \exp\left(-\alpha_{N_c+1}^2\right) c_m \quad \text{for} \quad m \leq N_c \qquad \text{(B3)}$$

In this way we have demonstrated that the product

$$\mathcal{V}^2 c_m = \text{const.} \quad \text{for} \quad m \leq N_c, \qquad \text{(B4)}$$

that is, it does not change under the shift of the cut-off.

As second step, we demonstrate that the latter property implies that the product $\mathcal{V}^2 G(s)$ is also invariant at low frequency. Similarly as in Appendix A, $G(s)$ has a natural time-scale separation between the (slow) dynamics of the phase and the (fast) dynamics of the oscillators at high-frequency. At low frequency $s \ll \omega_c = N_c\delta\omega$, we can approximate the product

$$\mathcal{V}^2 G(s) = \sum_{m=0}^{\infty} \frac{\mathcal{V}^2 c_m s}{s^2 + \omega_m^2} \approx \sum_{m=0}^{N_c} \frac{(\mathcal{V}^2 c_m)s}{s^2 + \omega_m^2}, \qquad \text{(B5)}$$

since $s \ll \omega_m$ and the coefficients c_m also decrease for $m > N_c$. Because the low-frequency form of $G(s)$ involves only the coefficients c_m with $m \leq N_c$, the product $\mathcal{V}^2 G(s)$ is indeed invariant under a variation of the frequency cut-off.

[1] J. E. Mooij, T. P. Orlando, L. Levitov, L. Tian, C. H. v. d. Wal, and S. Lloyd, Science **285**, 1036 (1999).
[2] I. M. Pop, I. Protopopov, F. Lecocq, Z. Peng, B. Pannetier, O. Buisson, and W. Guichard, Nature Phys. **6**, 589 (2010).
[3] I. M. Pop, B. Douçot, L. Ioffe, I. Protopopov, F. Lecocq, I. Matei, O. Buisson, and W. Guichard, Phys. Rev. B **85**, 094503 (2012).
[4] V. E. Manucharyan, J. Koch, L. I. Glazman, and M. H. Devoret, Science **326**, 113 (2009).
[5] V. E. Manucharyan, N. A. Masluk, A. Kamal, J. Koch, L. I. Glazman, and M. H. Devoret, Phys. Rev. B **85**, 024521 (2012).
[6] V. E. Manucharyan, J. Koch, M. Brink, L. I. Glazman, and M. H. Devoret, arXiv:0910.3039 (2009).
[7] O. V. Astafiev, L. B. Ioffe, S. Kafanov, Y. A. Pashkin, K. Y. Arutyunov, D. Shahar, O. Cohen, and J. S. Tsai, Nature **484**, 355 (2012).
[8] J. T. Peltonen, O. V. Astafiev, Y. P. Korneeva, B. M. Voronov, A. A. Korneev, I. M. Charaev, A. V. Semenov, G. N. Golt'sman, L. B. Ioffe, T. M. Klapwijk, and J. S. Tsai, Phys. Rev. B **88**, 220506(R) (2013).
[9] J. S. Lehtinen, K. Zakharov, and K. Y. Arutyunov, Phys. Rev. Lett. **109**, 187001 (2012).
[10] T. P. Orlando, J. E. Mooij, L. Tian, C. H. van der Wal, L. S. Levitov, S. Lloyd, and J. J. Mazo, Phys. Rev. B **60**, 15398 (1999).
[11] J. E. Mooij and C. J. P. M. Harmans, New J. Phys. **7**, 219 (2005).
[12] J. E. Mooij and Y. V. Nazarov, Nature Phys. **2**, 169 (2006).
[13] K. Matveev, A. Larkin, and L. Glazman, Phys. Rev. Lett. **89**, 096802 (2002).
[14] A. M. Hriscu and Y. V. Nazarov, Phys. Rev. Lett. **106**, 077004 (2011).
[15] A. M. Hriscu and Y. V. Nazarov, Phys. Rev. B **83**, 174511 (2011).
[16] M. Vanević and Y. V. Nazarov, Phys. Rev. Lett. **108**,

187002 (2012).
[17] G. Rastelli, I. M. Pop, and F. W. J. Hekking, Phys. Rev. B **87**, 174513 (2013).
[18] H. P. Büchler, V. B. Geshkenbein, and G. Blatter, Phys. Rev. Lett. **92**, 067007 (2004).
[19] R. Süsstrunk, I. Garate, and L. I. Glazman, Phys. Rev. B **88**, 060506 (2013).
[20] L. B. Ioffe, M. V. Feigel'man, A. Ioselevich, D. Ivanov, M. Troyer, and G. Blatter, Nature **415**, 503 (2002).
[21] L. B. Ioffe and M. V. Feigel'man, Phys. Rev. B **66**, 224503 (2002).
[22] S. Gladchenko, D. Olaya, E. Dupont-Ferrier, B. Douçot, L. B. Ioffe, and M. E. Gershenson, Nature Phys. **5**, 48 (2009).
[23] W. Guichard and F. W. J. Hekking, Phys. Rev. B **81**, 064508 (2010).
[24] K. C. Wright, R. B. Blakestad, C. J. Lobb, W. D. Phillips, and G. K. Campbell, Phys. Rev. Lett. **110**, 025302 (2013).
[25] L. Amico, D. Aghamalyan, H. Crepaz, F. Auksztol, R. Dumke, and L.-C. Kwek, Sci. Rep. **4** (2014), 10.1038/srep04298.
[26] J. S. Langer and V. Ambegaokar, Phys. Rev. **164**, 498 (1967); D. E. McCumber and B. I. Halperin, Phys. Rev. B **1**, 1054 (1970).
[27] N. Giordano, Phys. Rev. Lett. **61**, 2137 (1988).
[28] A. D. Zaikin, D. S. Golubev, A. van Otterlo, and G. T. Zimányi, Phys. Rev. Lett. **78**, 1552 (1997).
[29] K. Arutyunov, D. Golubev, and A. Zaikin, Phys. Rep. **464**, 1 (2008).
[30] A. Bezryadin, C. N. Lau, and M. Tinkham, Nature **404**, 971 (2000).
[31] C. N. Lau, N. Markovic, M. Bockrath, A. Bezryadin, and M. Tinkham, Phys. Rev. Lett. **87**, 217003 (2001).
[32] J. S. Lehtinen, T. Sajavaara, K. Y. Arutyunov, M. Y. Presnjakov, and A. L. Vasiliev, Phys. Rev. B **85**, 094508 (2012).
[33] C. Cirillo, M. Trezza, F. Chiarella, A. Vecchione, V. P. Bondarenko, S. L. Prischepa, and C. Attanasio, Appl. Phys. Lett. **101**, 172601 (2012).
[34] T. T. Hongisto and A. B. Zorin, Phys. Rev. Lett. **108**, 097001 (2012).
[35] P. Li, P. M. Wu, Y. Bomze, I. V. Borzenets, G. Finkelstein, and A. M. Chang, Phys. Rev. Lett. **107**, 137004 (2011).
[36] T. Aref, A. Levchenko, V. Vakaryuk, and A. Bezryadin, Phys. Rev. B **86**, 024507 (2012).
[37] M. W. Brenner, D. Roy, N. Shah, and A. Bezryadin, Phys. Rev. B **85**, 224507 (2012).
[38] M. Singh and M. H. W. Chan, Phys. Rev. B **88**, 064511 (2013).
[39] A. Murphy, P. Weinberg, T. Aref, U. C. Coskun, V. Vakaryuk, A. Levchenko, and A. Bezryadin, Phys. Rev. Lett. **110**, 247001 (2013).
[40] C. H. Webster, J. C. Fenton, T. T. Hongisto, S. P. Giblin, A. B. Zorin, and P. A. Warburton, Phys. Rev. B **87**, 144510 (2013).
[41] Y. Makhlin, G. Schön, and A. Shnirman, Rev. Mod. Phys. **73**, 357 (2001).
[42] M. H. Devoret, A. Wallraff, and J. M. Martinis, arXiv:cond-mat/0411174 (2004).
[43] J. Clarke and F. K. Wilhelm, Nature **453**, 1031 (2008).
[44] C. H. van der Wal, A. C. J. ter Haar, F. K. Wilhelm, R. N. Schouten, C. J. P. M. Harmans, T. P. Orlando, S. Lloyd, and J. E. Mooij, Science **290**, 773 (2000).
[45] F. K. Wilhelm, C. H. van der Wal, A. C. J. ter Haar, R. N. Schouten, C. J. P. M. Harmans, J. E. Mooij, T. P. Orlando, and S. Lloyd, Physics-Uspekhi **44**, 117 (2001).
[46] I. Chiorescu, Y. Nakamura, C. J. P. M. Harmans, and J. E. Mooij, Science **299**, 1869 (2003).
[47] A. J. Leggett and A. Garg, Phys. Rev. Lett. **54**, 857 (1985).
[48] A. J. Leggett, Journal of Physics: Condensed Matter **14**, R415 (2002).
[49] J. R. Friedman, V. Patel, W. Chen, S. K. Tolpygo, and J. E. Lukens, Nature **406**, 43 (2000).
[50] A. J. Leggett, S. Chakravarty, A. T. Dorsey, M. P. A. Fisher, A. Garg, and W. Zwerger, Rev. Mod. Phys. **59**, 1 (1987).
[51] U. Weiss, *Quantum Dissipative Systems*, 4th ed. (World Scientific Publishing, Singapore, 2012).
[52] H. Breuer and F. Petruccione, *The Theory of Open Quantum Systems* (Oxford University Press, Oxford, 2007).
[53] A. O. Caldeira and A. J. Leggett, Phys. Rev. Lett. **46**, 211 (1981).
[54] F. Nesi, E. Paladino, M. Thorwart, and M. Grifoni, Phys. Rev. B **76**, 155323 (2007).
[55] H. Spohn and R. Dümcke, J. Stat. Phys. **41**, 389 (1985).
[56] C. Aslangul, N. Pottier, and D. Saint-James, J. Phys. France **47**, 1657 (1986).
[57] H. Dekker, Phys. Rev. A **35**, 1436 (1987).
[58] D. Porras, F. Marquardt, J. von Delft, and J. I. Cirac, Phys. Rev. A **78**, 010101 (2008).
[59] S. E. Korshunov, Sov. Phys. JETP **63**, 1242 (1986).
[60] S. E. Korshunov, Sov. Phys. JETP **68**, 609 (1989).
[61] N. A. Masluk, I. M. Pop, A. Kamal, Z. K. Minev, and M. H. Devoret, Phys. Rev. Lett. **109**, 137002 (2012).
[62] M. T. Bell, I. A. Sadovskyy, L. B. Ioffe, A. Y. Kitaev, and M. E. Gershenson, Phys. Rev. Lett. **109**, 137003 (2012).
[63] U. Weiss and H. Grabert, Phys. Lett. A **108**, 63 (1985).
[64] U. Weiss, H. Grabert, P. Hänggi, and P. Riseborough, Phys. Rev. B **35**, 9535 (1987).
[65] S. E. Korshunov, Sov. Phys. JETP **66**, 872 (1987).
[66] D. Averin, Y. Nazarov, and A. Odintsov, Physica B: Cond. Mat. **165**, 945 (1990).
[67] G. Schön and A. D. Zaikin, Physics Reports **198**, 237 (1990).
[68] F. W. J. Hekking and L. I. Glazman, Phys. Rev. B **55**, 6551 (1997).
[69] A. J. Leggett, Phys. Rev. B **30**, 1208 (1984); S. Chakravarty and A. Schmid, *ibid.* **33**, 2000 (1986).
[70] M. Tinkham, *Introduction to Superconductivity*, 2nd ed. (McGraw-Hill, New York, 1996).
[71] S. E. Nigg, H. Paik, B. Vlastakis, G. Kirchmair, S. Shankar, L. Frunzio, M. H. Devoret, R. J. Schoelkopf, and S. M. Girvin, Phys. Rev. Lett. **108**, 240502 (2012).
[72] D. G. Ferguson, A. A. Houck, and J. Koch, Phys. Rev. X **3**, 011003 (2013).
[73] B. Peropadre, D. Zueco, F. Wulschner, F. Deppe, A. Marx, R. Gross, and J. J. García-Ripoll, Phys. Rev. B **87**, 134504 (2013).